

## Field annealed closed-path fluxgate sensors made of metallic-glass ribbons.

Pavol Butvin<sup>1</sup>, Michal Janošek<sup>2</sup>, Pavel Ripka<sup>2</sup>, Beata Butvinová<sup>1</sup>, Peter Švec Sr<sup>1</sup>,  
Marek Kuzminski<sup>3</sup>, Peter Švec Jr<sup>1</sup>, Dušan Janičkovič<sup>1</sup>, Gabriel Vlasák<sup>1</sup>

*1 Institute of Physics, Slovak Academy of Sciences, 845 11 Bratislava, Slovakia*

*2 Czech Technical University in Prague, 166 27 Praha, Czech Republic*

*3 Institute of Physics, Polish Academy of Sciences, 02-668 Warszawa, Poland*

### Abstract

---

The possibilities to improve the performance of certain fluxgate sensor types are still not exhausted. Two types of closed-path sensors – ring core and racetrack – were checked to reveal risky combination of material and construction parameters, and means to optimize the combination were tested. One-step field annealing of Co-based metallic glass was chosen to acquire low-magnetostrictive material with anisotropy required to reduce noise by favoring magnetization rotation. Locally misaligned anisotropy promoted incoherent rotation and handicapped racetrack noise performance. Despite the risk of bending stress aggravated by small – 12 mm - diameter, the ring cores fared better and reproducibly achieved noise  $7 \text{ pT} / \sqrt{\text{Hz}} @ 1\text{Hz}$  when thoroughly fixed and annealed in an optimal sheath. As far as we know these are the lowest noise values achieved for this size of fluxgate sensors.

---

### 1. Introduction

Fluxgate sensors (magnetometers) are still the first choice when an accurate directional measurement of low-frequency medium intensity magnetic field should be performed without the need of shielding and cryogenic temperatures. Properties of the magnetic core material and its impact on sensor performance are the main scope of this work. Magnetic anisotropy together with its response to the induction method and material handling appears to be the most important property linked to the most haunted performance parameter – the noise. Extended experience (e.g. [1, 2]) suggests preferring materials with low magnetostriction [1] and low Curie temperature [3]. Co-Cr-Fe-B-Si metallic glass fulfills the demands well. Since the noise (Barkhausen noise) comes from abrupt changes of magnetic flux, it is most often attributed to an abrupt domain-wall movement and several methods to suppress it are applied [4]. Induction of strong transversal anisotropy by stress annealing came to be the first choice for metallic glasses [1] to promote the magnetization rotation to the detriment of wall movement. Nevertheless, there are inherent limitations for the tape-wound ring cores, since for the anisotropy to be uniform it has to be induced in the straight ribbon prior to winding the core. Then the ribbon is submitted to additional bending stress at core winding. The magnetostriction desired here to be zero is still tricky due to its variation with the stress [5]. To avoid this problem, we chose field annealing that enables a tape-wound core to relax significant part of the bending stress. The sensor electronics used in tested prototypes adheres to the standard principles of bipolar AC excitation and evaluation of the output signal at its second harmonic frequency. Two forms of magnetic cores were used: true closed path racetrack and tape-wound toroid with a mean field path of 3 to 6 cm. It should be emphasized that the diameter of the used tape-wound ring-cores is 10-mm or 12-mm, which is less than the commonly used dimensions (17-25 mm diameter). The choice of these dimensions was

given by demands for miniaturization by simultaneously keeping the good noise properties. However, the small diameter amplifies not only the bending-stress related problems, but also the symmetry issues in miniature ring-cores – the sensitivity to any 2<sup>nd</sup> harmonic distortion of the excitation current is high.

### 1.1 Field annealing

Magnetic anisotropy with easy magnetization axis directed transversally to the field direction is widely used not to excite domain-wall movement that easily tends to be irregular and generate noise. The simplicity of the task to provide domain walls minimally sensitive to directional external field ends at the requirement of domains and 180° walls to be oriented perpendicularly to the field. Apparently, the anisotropy should be strong. But strong anisotropy (with large coefficient  $K_u$ ) results in fine domains [6, 7] and so in many walls. This accentuates the demand of domain-structure homogeneity not to provide any misaligned walls. The anisotropy induced by stress annealing in Co-based metallic glasses is generally stronger [8, 9] than the anisotropy by field annealing and can be, contrary to field annealing, further promoted by specific pre-annealing of the ribbon. However, the homogeneity of stress-annealing anisotropy meets with more limitations [10, 11]. Apart from the necessity to risk severe inhomogeneity when annealing a ringcore or at least bending stress when wrapping annealed straight ribbon, the anisotropy energy is sensitive to the actual local stress applied during annealing. Due to problems with ribbon cross section geometry and the rather rough surface, it is difficult to keep the stress uniform. The annealing temperature requires a compromise too. Stress annealing uses higher temperature and often a preannealing to minimize magnetostriction coefficient [1]. Field annealing is principally limited to be performed below the Curie temperature and we did not consider looking for a simultaneous manipulation of magnetostriction. Nevertheless, field annealing omits one technological step (preannealing) and induces some domain wall stabilization [12] that is useful when low wall mobility and high start field is desired.

## 2. Experimental

Amorphous ribbons of  $\text{Co}_{67}\text{Cr}_7\text{Fe}_4\text{B}_{13}\text{Si}_9$  alloy (#1) were prepared by planar-flow casting on air. To achieve modest difference of the Curie temperature  $T_C$ , 1 at.% of Cr was substituted by Mn in the reference alloy #2. The composition of ribbons was checked by ICP AES method. We used ribbons with 2.6/0.018 and 20/0.022 mm width/thickness. Racetracks (RT) were chemically etched from the 20 mm wide ribbon #2 center to give 2-mm width and  $30 \times 10 \text{ mm}^2$  outer footprint (Fig. 1). The ring cores - toroids (TOR) were wound with 5 to 10 wraps into 10 mm inner diameter PEEK sheaths (Fig. 1). The ribbon was not glued or fixed in other means. Later, the ring cores were wound also into MACOR sheaths with 12-mm inner diameter, which were composed from two parts glued together, where the final gap for the core was 0.2mm reducing the spring-effect of the ribbon to minimum.

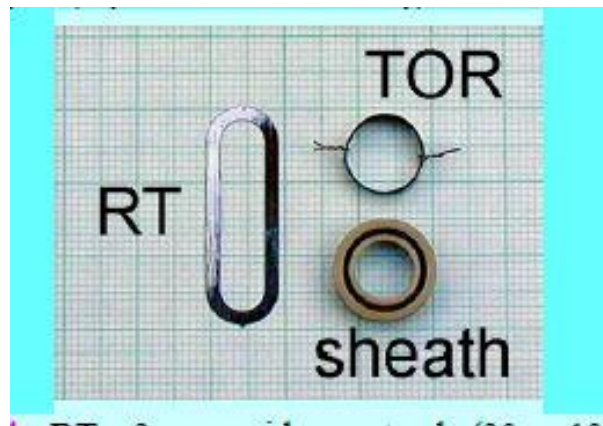


Fig. 1. Actual size ring core (TOR) and racetrack (RT) photographed on millimeter-scaled paper. The bare core was prior to inserting into sheath secured by makeshift wire fixture since no glue or welding was used. PEEK “slack” sheath is shown.

The standard field annealing used one temperature (250° or 265°C) with the isotherm duration of 120 or 90 minutes and was performed in Ar atmosphere under ~10 kA/m transversal external field. Hysteresis loops were recorded on a digitizing hysteresisgraph where the sensors were excited by sine signal from a low-output-impedance amplifier. The energy density of hard-ribbon-axis (HRA) anisotropy (Table 1.) has been evaluated from saturation – remanence – loop outer cut-off area in 1<sup>st</sup> and 3<sup>rd</sup> quadrants. The noise parameters were measured in a standard fluxgate-sensor configuration with transformer—coupled, parallel-tuned excitation tank with 12-kHz driving frequency and variable excitation amplitude up to 10 kA/m p-p. The excitation winding had 120-turns of 0.2-mm-dia wire and the pickup-coil had 180-turns tuned by parallel capacitor at 2<sup>nd</sup> harmonic. A lock-in amplifier SR830 was used for the 2<sup>nd</sup> harmonic detection, its digital output was evaluated in the noise measurements. Domain structure was imaged by polarization microscope exploiting the magneto-optical Kerr effect (MOKE). Major domain magnetization direction is identified by contrast: full contrast is obtained when maximum magneto-optical sensitivity of the microscope is parallel or anti-parallel to domain magnetization. Curie temperature was determined by thermogravimetry. Etched-out circular samples were used to determine magnetostriction coefficient  $\lambda_s$  by calculating it from sample strain measured by a capacitance method.

### 3. Results and discussion

Table 1

Magnetic parameters of Co-based metallic glass ribbons used in fluxgate sensor cores.

Material & condition	Magnetostriction $\lambda_s$	Curie temp. $T_c$ [°C]	Saturation Bs [T]	HRA anisotropy [J/m <sup>3</sup> ]	Permeability $\mu_{eff}$	Noise spect. density [pTrms/ $\sqrt{Hz}$ ] @ 1Hz	
						RT	TOR
#1 as-cast	-5.2 e-7	270	0.53	~ 0	-	-	10
#1 annealed	-6.0 e-7	282	0.55	22	6800	-	5
#2 as-cast	-2.0 e-7	282	0.61	11	16400	8	10
#2 annealed	-5.0 e-7	291	0.63	31	5600	70	8

The higher- $T_C$  ribbon #2 is a 20mm wide ribbon. When measured as full-width strip or in the etched racetrack geometry it shows slightly slant loop (HRA anisotropy  $\sim 11 \text{ J/m}^3$ ) already in the as-cast state unlike ribbon #1 (see Fig.2a). It appears that the bending stress  $\sigma$  slightly lowers the HRA anisotropy despite of as-cast or annealed state – the loops of #2 TORs are less slant and/or display a steep low-field part (Fig. 2b). The culprit of the as-cast HRA anisotropy could be the as-cast structural anisotropy [13] or a creep anisotropy induced by intrinsic macroscopic stress acting in the still hot “fresh” ribbon at the end of casting. Similar resulting anisotropy is observed after no-intentional-stress annealing in some Fe-Nb-Cu-B-Si ribbons with the same sign of creep-induced anisotropy [14]. In any case, the as-cast-borne magnetic anisotropy is not homogeneous and it comprises, apart from HRA, an easy-ribbon-axis (ERA) component too.

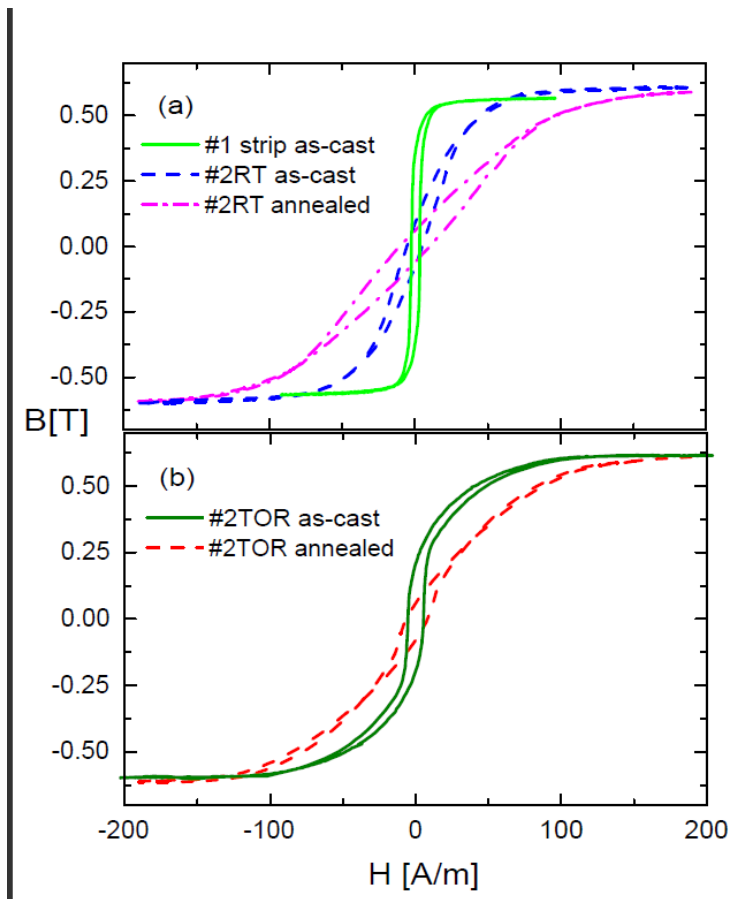
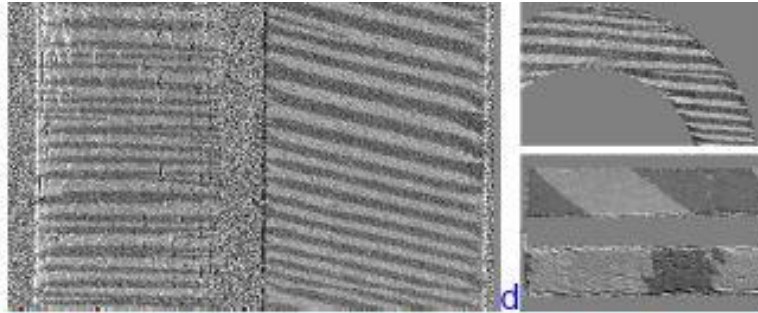


Fig. 2. Loops (1 kHz) of differently shaped samples of material #2. Loop for as-cast material #1 is plotted as reference to show different as-cast anisotropy without additional bending stress (therefore strip sample). Indicated samples were annealed at  $265^\circ\text{C}$  for 90 minutes

The persisting ERA component prevents the domains to align perfectly transversally to the ribbon axis after the field annealing (see Fig. 3b). This is not the case of narrow ribbon #1 with its upright as-cast loop (Fig. 2a and 3a). As seen by comparison of #1 loops in Figs 2a and 2b, bending stress acting through magnetoelastic interaction induces the coexistence of HRA and ERA components. The stress appears to support preferentially the already present ERA component in ribbon #2. This is seen well by comparing Figs 3b and 3d. Since the strips of #2 were longitudinally cut to match the width and demagnetization factor of the narrower

#1 and the domain tilt ( $10^\circ$  from transverse) is slightly greater than for etched RT (Fig. 3c -  $\sim 5^\circ$  tilt), one can suspect remnants of shear stress to assist the ERA anisotropy component. However, the comparison of adjacent cut narrow strips with the genuine-width (20 mm) strip of ribbon #2 showed only minor differences ( $\pm 1 \text{ J/m}^3$ ) of the HRA anisotropy. This excludes a residual stress possibly induced by cutting as the reason of the observed tilt of transversal domains. Moreover the comparison shows that the field used at the field annealing saturated the ribbon transversally and did not allow different demagnetization factor to show up on 20 mm down to 2.6 mm wide ribbons.



**Fig.3** Domain patterns of field annealed samples: a- #1 genuine width 2.6 mm, b- #2 cut to 3 mm width, c- #2 RT (reduced) d- bent #2 (MMOS vertical)

*Fig. 3. Domain patterns of equally field-annealed samples: (a) – full genuine width strip of ribbon #1 (left) and cut-width strip of #2 (right), (b) – RT (half the magnification of (a) or (c)), (c)- strip of #2 bent to TOR curvature after being annealed as straight strip: no external field (upper) and vertical bias field applied (lower). Ribbon axis always vertical, major domain magnetization horizontal for (a), (b), vertical for (c).*

Figures 2a and 2b and especially Fig. 3d point to the bending stress as the major risk factor, which deteriorates a tilted linear loop and supports unwanted ERA anisotropy component despite of low material magnetostriction. Clear difference is seen in Fig.4 to come from additional (applied after annealing) bending stress. The additional bending stress also disturbs the domain wall stabilization as seen by comparison of Figs 3b and 3d – the walls and domains visibly tilt by bending and still more tilted by longitudinal external field, the walls move easily. Different response to longitudinal field is observed without bending – it will be commented below at RT – TOR comparison.

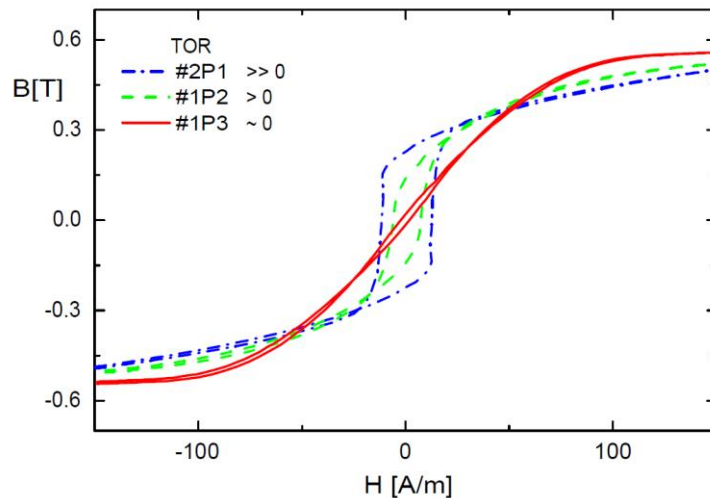


*Fig. 4. Loops (40 Hz) of equally field-annealed (2h at 250°C) ring cores wound of equally long ribbon sections. Whereas #1P3 ring core was annealed and measured within the 10 mm-diameter sheath, the #1P2 and #2P1 ring cores were annealed as ~30 mm-diameter rings but measured inserted into equal 10 mm diameter sheaths (after thorough diameter reduction). Note that ribbon #2 is ~20% thicker than #1.*

Nevertheless, the bending stress in ring cores might not to be relaxed enough at below- $T_C$  temperatures used at the annealing, although the “zero additional stress” loop (Fig. 4 – TOR #1P3) is already looking fine. Fig. 5a shows the comparison of field-annealed 5-wrap cores in MACOR tight sheaths (TOR #1M4) and 10-wrap core in PEEK slack sheath (TOR #1P3). The comparison was intended to identify whether the different thermal expansion of MACOR and the ribbon does not cause significant thermal stress in the core to show up consequences to the resulting anisotropy. The small difference seen between the corresponding loops does not clearly represent either the slightly different annealing or a thermal stress result. The difference rather reflects somewhat poorer reproducibility of cores annealed in slack PEEK sheaths. Three cores wound of consecutive ribbon sections and annealed in the “taut” MACOR sheaths (#1M4 is a member of the trinity) responded with practically matching loops. To test further the residual-stress suspicion, differently wound field-annealed ring cores were measured and then released from the sheath to see whether they reveal residual stress by partial unwrapping. Relatively special portion of the ribbon – bulging notably the wheel side out – has been chosen and one of the two cores - #1P4 -was wound air-side up and the other - #1P5 - wheel-side up. Notable difference is observed between the loops – Fig.5b. Unwrapping showed up different too – the wheel-side-up core unwrapped to four times larger diameter when pulled out from the sheath whereas the air-side-up core merely doubled its diameter. One can conclude that the 265°C annealing temperature is not enough to relax the bending stress completely and if the core is wound wheel-side up, the residual stress appears still larger. Unfortunately, we are so far not able to recognize for sure, which effects are responsible for the low-field bellies on loops of Fig. 5b.

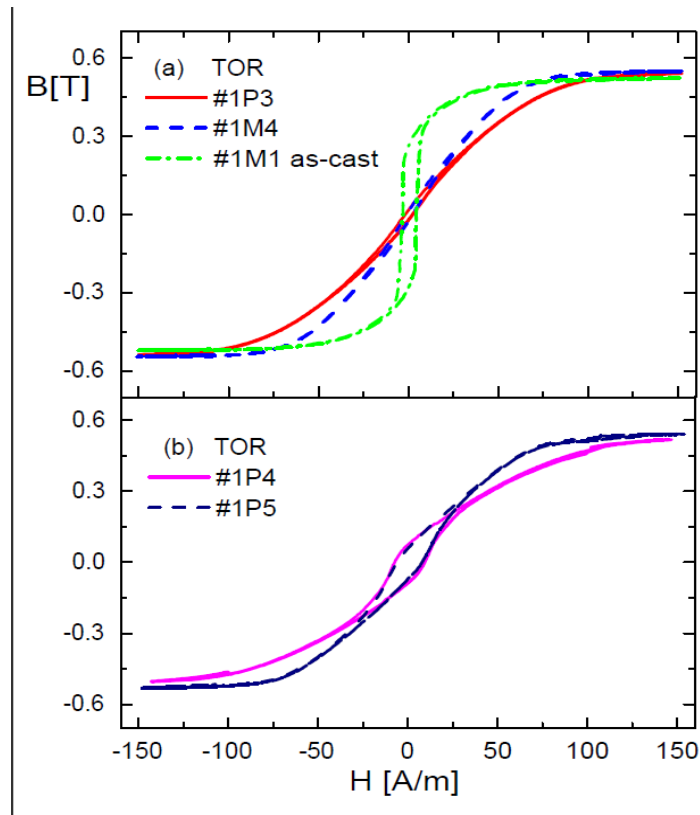


Fig.5. Loops (200 Hz) of differently treated ring cores in different sheaths (P for PEEK, M for MACOR). (a) – #1M4 represents well-reproducible “taut” sheath cores field-annealed at 265°C compared to as-cast core #1M1 to show acquired anisotropy and to the best of “slack” sheath cores annealed at 250°C. (b) – equally annealed (265°C) but differently wound cores: #1P4 ribbon air side up, #1P5 wheel side up.”

### 3.1 Comparison of racetracks to toroidal cores (RT –TOR).

The most obvious difference between TOR and RT is the advantage of the latter to avoid bending stress easily. Fig. 6 however shows the principal risks of a field-annealed racetrack: The U-turn part shows easy direction along the sensor exciting field, which promotes domain wall movement. Moreover, there are remnants of incoherent rotation over the whole RT – the medium black density indicates distinct areas magnetized approximately perpendicular to magneto-optical sensitivity, thus parallel to the exciting field whereas the rest area is still controlled by the induced transverse anisotropy. Due to experimental limitation – external field is directed like field to be measured, not sensor exciting field - Fig. 6 does not display the expected marked domain wall movement in U-turn part. Nonetheless we observed easy wall movement on no-field-annealed straight strip samples if external field was applied along the annealing-stabilized walls (not shown). Thus the wall stabilization significantly hampers their movement under large-angle external field, but is not efficient enough to block the wall movement under low-angle field. Recalling Fig. 2a, the RT drawbacks appear to correlate to the low-field “belly” on the loop in annealed RT. If compared to TOR, field-annealed RT performed worse (loops, noise) with slightly better as-cast results.



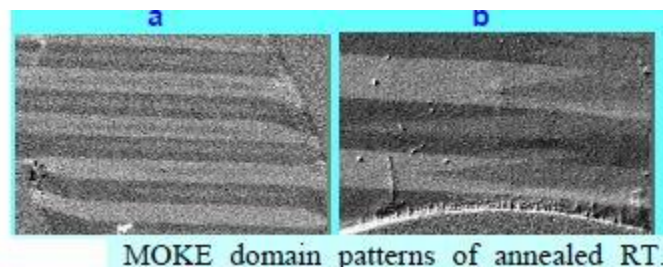


Fig. 6. Domain patterns of field-annealed RT of #2. Note 3-level black density – the medium one identifies areas magnetized at a large angle to horizontally magnetized majority domains. Left – weak vertical ac demagnetizing field leaves large-angle-magnetized domains on straight parts of RT. Right – 4x stronger field still leaves the domains on U-turn parts (but straight parts show horizontally magnetized domains only – not shown). Magnification is equal for left and right image.

### 3.2 Noise performance

The noise performance of TOR and RT as well appears clearly to correlate with the loop shape: Worse noise comes with the more pronounced low-field steep part (“belly”) of the loop. This is seen clearly if Fig 7 is compared to the loops (Fig. 4). According to previous paragraphs, we ascribe the deterioration of a slim linear loop to domain wall movement and/or incoherent rotation promoted mainly by (additional) bending stress.

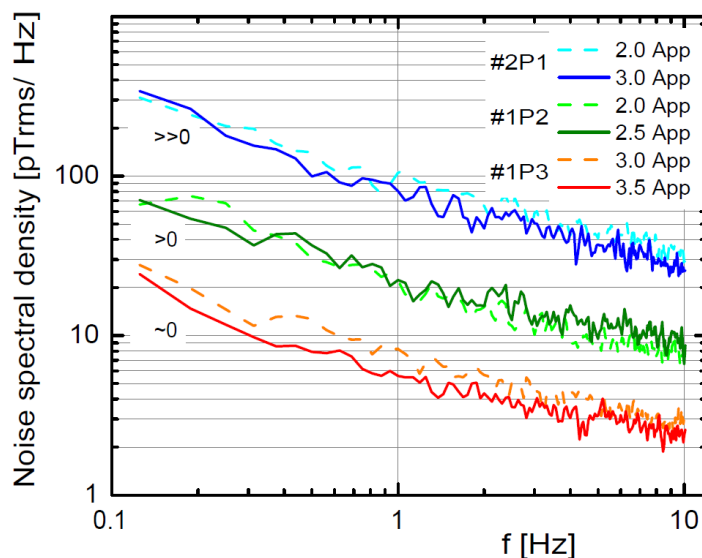


Fig. 7. Noise of FG sensors made of field-annealed ring cores (the same as in Fig. 4.). Excitation field (12 kHz) scales linearly with the current quoted in the legend. Here the best noise figure - 5 pT /  $\sqrt{\text{Hz}}$  @ 1Hz is shown by TOR #1P3

Then the loops of Fig. 5 (differently wound cores) can be correlated to the noise results too: At 3 A<sub>p-p</sub> excitation (10 kA/m p-p), the noise at 1 Hz amounts to 40, 30, 6.7 pT /  $\sqrt{\text{Hz}}$  for TOR



#1P5, #1P4, #1M4 respectively. One comment for the higher- $T_C$  material #2: It never showed lower noise than #1 – the best sensor of #2 ring cores presented noise around  $12 \text{ pT} / \sqrt{\text{Hz}} @ 1 \text{ Hz}$ , though at still larger excitation current of  $4 \text{ A}_{\text{p-p}}$  (not shown). The large noise figures for poorly fixed ring cores point to still another factor – a stray field, which deteriorates the field symmetry and adds to the (residual) bending stress effect. Large free space was left within the PEEK sheath slot so the cores #1P4 and #1P5 were able to move their wraps. (Wide slot aided the core withdrawal. We did not use any supporting springs.) The non-symmetric stray field can come from the ribbon ends with mismatched overlap, but is more probable to come from inhomogeneous bending stress along the core circumference, causing excessive noise. The noise of this sensor in a practical fluxgate mode could be higher also because of the large zero-field feedthrough due to core inhomogeneity, which compromised dynamic range of the second harmonic detector [15]. The poor symmetry also promotes the effect of any 2<sup>nd</sup> harmonic appearing in the excitation current. Better noise reduction by transversal field annealing is achieved in TOR if compared to RT (see Table). However TORs come with more, though avoidable risks – the bending stress and poorer symmetry. If ring cores are prepared thoroughly, the results are good and well reproducible. The slim linear loops displayed in Figs 4 and 5a come from well-fixed and comprehensively wound ring cores. Reproducibility test with 5-wrap TORs (#1M2÷4) reveals equal loops and equally low noise ( $\sim 7 \text{ pT} / \sqrt{\text{Hz}} @ 1 \text{ Hz}$ ) for the three equally handled cores.

The large necessary excitation field poses already a limitation. The ensuing heating can compromise the parameter stability and it can disable the domain-wall stabilization, moreover it contributes to drift of sensor parameters. However we found it necessary for the current material to keep the saturation level deep enough to obtain low noise by applying the rule of thumb having 100x higher excitation level than the actual required field for saturation. When reaching this limit, the noise did not decrease any lower. The explanation assumed by Scouten [16] is based on macroscopic inhomogeneity in the ribbon, i.e. inclusions of magnetically hard regions. So far we have no noise-independent indication that this is the case with our ribbons. When compared to the results of Primdahl [17], we have to note that excitation level required for obtaining low noise in the case of field-annealed Co-Cr-Fe-B-Si ribbons is still higher than that for stress annealed Vitrovac 6025X used for the same purpose by the Danish group.

#### 4. Conclusions

The few degree difference in  $T_C$  of the two alike materials studied is not enough to assess the importance of low Curie temperature for fluxgate sensor performance. However, low  $T_C$  poses certain risk for field-annealed ring cores not to provide optimal residual bending stress relaxation. The noise of field-annealed racetrack tapes was found higher after field-annealing due to the presence of longitudinal anisotropy in the U-shaped ends of the racetrack, which is inherent to the geometry. If we conclude the progress for the 10/12-mm ring-cores, we can state that:

- The potential of rapidly quenched ribbons for use in FG sensors is still not exhausted.
- Field annealing is a viable and competitive option to promote the desired magnetization rotation provided by transversal anisotropy in order to reduce Barkhausen noise. It also allows to field-anneal an already finished core-sheath assembly, possibly lowering the manufacturing costs and release the bending stress
- Despite problems with ribbon free ends and high sensitivity to even harmonics in the excitation, the major difficulty of ring cores with small diameters - bending stress - can be

## Preprint

Butvin, P.B. - Janošek, M. - Ripka, P. - Butvinová, B.B. - Švec sr., P.Š. - et al.: Field Annealed Closed-path Fluxgate Sensors Made of Metallic-glass Ribbons In: Sensors and Actuators. 2012, vol. 2012, no. 184, p. 72-77. ISSN 0924-4247.

sufficiently reduced by field annealing to enable sensor noise as low as  $5 \text{ pT}/\sqrt{\text{Hz}}$  @ 1 Hz. According to our knowledge, these are the lowest noise figures achieved for fluxgate sensors of this size.

## Acknowledgments

The authors are grateful for partial financial support by APVV grant SK-CZ -0078-11. Slovak authors thank also to VEGA grants No 2/0056/11, 2/0111/11 and to FUN-MAT Center of Excellence. Czech authors thank also to Grant No. TA01010298 by the Technology Agency of the Czech Republic.

## Preprint

Butvin, P.B. - Janošek, M. - Ripka, P. - Butvinová, B.B. - Švec sr., P.Š. - et al.: Field Annealed Closed-path Fluxgate Sensors Made of Metallic-glass Ribbons In: Sensors and Actuators. 2012, vol. 2012, no. 184, p. 72-77. ISSN 0924-4247.

## References:

- [1] O.V. Nielsen, P. Brauer, F. Primdahl, T. Risbo, J.L. Jørgensen, C. Boe, M. Deyerler, S. Bauereisen, A high-precision triaxial fluxgate sensor for space applications: layout and choice of materials, *Sens. Actuators A* 59 (1997) 168-176.
- [2] P. Ripka, Advances in fluxgate sensors, *Sens. Actuators A* 106 (2003) 8-14.
- [3] K. Shirae, Noise in amorphous magnetic materials, *IEEE Trans. Magn.* 20 (5) (1984) 1299-1301.
- [4] S.B. Ubizskii, L.P. Pavlyk, The pendulum-like fluxgate magnetic field sensor, *Sens. Actuators A* 141 (2008) 440-446.
- [5] A. Siemko, H.K. Lachowicz, Comments on the indirect measurement of magnetostriction in low-magnetostrictive metallic glasses, *J. Magn. Magn. Mater.* 66 (1987) 31-36.
- [6] J.D. Livingston, W.G. Morris, T. Jagielinski, Effects of anisotropy on domain structures in amorphous ribbons, *IEEE Trans. Magn.* 19 (1983) 1916-1918.
- [7] A. Hubert, R. Schäfer, *Magnetic Domains: The Analysis of Magnetic Microstructures*, Springer-Verlag, Berlin, 1998.
- [8] O.V. Nielsen, Effects of longitudinal and torsional stress annealing on the magnetic anisotropy in amorphous ribbon materials, *IEEE Trans. Magn.* 21 (1985), 2008-2013.
- [9] K. Závěta, O.V. Nielsen, K. Jurek, A domain study of magnetization processes in a stress-annealed metallic glass ribbons for fluxgate sensors, *J. Magn. Magn. Mater.* 117 (1992) 61-68.
- [10] J.D. Livingston, W.G. Morris, Magnetic domains on amorphous metal ribbons, *J. Appl. Phys.* 57 (1) (1985) 3555-3559.
- [11] F. Alves, R. Barrué, Anisotropy and domain patterns of flash stress-annealed soft amorphous and nanocrystalline alloys, *J. Magn. Magn. Mater.* 254-255 (2003) 155-157.
- [12] P. Butvin, B. de Ronzyová, Structural relaxation and domain wall stabilization in metallic glasses, *Z. Phys. Chem. Neue Folge*, 157 (1988) 329-333.
- [13] D. Spilsbury, P. Butvin, N. Cowlam, W.S. Howells, R.J. Cooper, Some evidence for "directional atomic pair ordering" in a cobalt-based metallic glass, *J. Mat. Sci. Eng. A* 226-228 (1997) 187-191.
- [14] B. Butvinová, P. Butvin, M. Kuzminski, M. Kadlečiková, A. Ślowska-Waniewska, Indication of intrinsic macroscopic forces affecting magnetic properties of Fe-Nb/Mo-Cu-B-Si ribbons, *IEEE Trans. Magn.* 48 (4) (2012) 1340-1343.
- [15] R. Petersen, F. Primdahl, B. Hernando, A. Fernandez, O.V. Nielsen, The ring core fluxgate sensor null feed-through signal, *Meas. Sci. Technol.* 8 (1992), 1149-1154
- [16] D.C. Scouten, Sensor noise in low-level flux-gate magnetometers, *IEEE Trans. Magn.* 8 (1972) 223-231.
- [17] O.V. Nielsen, J.R. Petersen, F. Primdahl, P. Brauer, B. Hernando, A. Fernandez, J.M.G. Merayo, P. Ripka, Development, Construction and Analysis of the "ØRSTED" Fluxgate Magnetometer, *Meas. Sci. Technol.* 6 (1995) 1099-1115